

GAS TARGET STUDIES  
AT THE  
NAVAL POSTGRADUATE SCHOOL  
LINEAR ACCELERATOR

Carter Dow Savage



United States  
Naval Postgraduate School



THESIS

GAS TARGET STUDIES AT THE  
NAVAL POSTGRADUATE SCHOOL LINEAR ACCELERATOR

by

Carter Dow Savage

Thesis Advisor:

F.R. Buskirk

June 1971

*Approved for public release; distribution unlimited.*

T139918

LIBRARY  
NAVAL POSTGRADUATE SCHOOL  
MONTEREY, CALIF. 93940

Gas Target Studies at the  
Naval Postgraduate School Linear Accelerator

by

Carter Dow Savage  
Ensign, United States Navy  
B.S., United States Naval Academy, 1970

Submitted in partial fulfillment of the  
requirements for the degree of

MASTER OF SCIENCE IN PHYSICS

from the

NAVAL POSTGRADUATE SCHOOL  
June 1971

thesis  
S217  
c.1

## ABSTRACT

A study of the parameters involved in electron scattering experiments with gaseous targets at the Naval Postgraduate School Linear Accelerator was conducted. The parameters included gas densities, effective target thicknesses, and radiative corrections to experimental cross-section calculations. To compare the NPGLINAC with other accelerators, an electron scattering experiment was performed, using a hydrogen-helium gas mixture target, at values of  $q^2$  from 0.10 to 0.55  $F^{-2}$ . The resulting charge form factor for helium was fairly consistent with previous experimental models; however, it was concluded that experiments using separate gas targets yield greater accuracy than those using a gas mixture.





## TABLE OF CONTENTS

I.	INTRODUCTION -----	7
	A. EXPERIMENTAL OBJECTIVES -----	7
	B. EXPERIMENTAL CALCULATIONS -----	10
II.	RADIATIVE CORRECTIONS -----	11
	A. BETHE-HEITLER CORRECTION -----	11
	B. THE SCHWINGER CORRECTION -----	15
III.	HELIUM FORM FACTOR -----	16
	A. INTRODUCTION -----	16
	B. THEORY -----	18
	C. EXPERIMENTAL METHOD -----	19
	1. Procedure -----	19
	2. Experimental Errors -----	20
	D. DATA REDUCTION -----	21
	1. Calculation of Cross Sections -----	21
	2. Error Analysis -----	25
	E. RESULTS AND CONCLUSIONS -----	26
APPENDIX A:	Frequently Used Constants -----	30
APPENDIX B:	Virial Coefficients -----	31
APPENDIX C:	Gas Target Effective Thickness -----	39
LIST OF REFERENCES	-----	42
INITIAL DISTRIBUTION LIST	-----	43
FORM DD 1473	-----	44



LIST OF TABLES

I. Effective Target Thickness ----- 14

II. Experimental He<sup>4</sup> Charge Form Factor ----- 27

III. Virial Coefficients for Several Gases  
at T = 77.32°K ----- 35

IV. Densities of Several Gases at Constant  
Temperature (77.32°K) for Various Pressures ----- 36



## LIST OF FIGURES

1. Gas Target Assembly -----	9
2. Spectrum of Elastically Scattered Electrons from He - H <sub>2</sub> Gas Mixture -----	22
3. Spectrum of Elastically Scattered Electrons from He - H <sub>2</sub> Gas Mixture -----	23
4. He <sup>4</sup> Charge Form Factor vs. $q^2$ -----	28
5. Temperature Bridge -----	38



## ACKNOWLEDGEMENT

The author wishes to express his sincere appreciation for the assistance rendered in preparation of this paper to Associate Professor Fred R. Buskirk. He also wishes to thank Capt. Louis P. Gaby, USAF, and Ens. Thomas W. Mader, USN, for their assistance in computer and calculator work.





## I. INTRODUCTION

### A. EXPERIMENTAL OBJECTIVES

The electron linear accelerator at the Naval Postgraduate School (NPGLINAC) has been in use since 1966, and has been described in theses by Barnett and Cunneen [Ref.1] and Midgarden [Ref.2]. Energy loss and nuclear structure experiments have been conducted using solid targets. In 1970, the scope of experimentation was broadened to include gas targets in addition to solid targets. While the technique of electron scattering measurements remained the same, there were several new problems to be considered when using gas targets instead of solid targets. Some of these problems included the following mechanical considerations:

- (a) Containers had to be designed to hold gases under high pressures.
- (b) A method of cooling the target area and keeping it at a constant temperature had to be designed and installed.
- (c) A method of feeding and evacuating the gas target chambers had to be devised, along with a method to measure the pressure inside the chamber.

The problem associated with high pressures and low temperatures arose because it was necessary to maintain the gases at high densities in order to obtain reasonable counting rates during experiments. Gases at atmospheric pressure and



temperature produced counting rates that were very low and much more time would have been required for a run.

These mechanical problems were solved by Professors Bumiller and Buskirk, Captain Louis Gaby, and the NPGLINAC technicians. A diagram depicting one of the gas target chamber arrangements is given in Figure 1.

Apart from the mechanical problems encountered when gas targets were introduced, several experimental problems also were evident. The experimental considerations included the following:

- (a) Effects of the target chamber windows on electron scattering experiments had to be determined.
- (b) The effective target thicknesses of gases had to be determined; i.e., only electrons scattered from a small part of the total volume of gas in the target chamber made their way into the spectrometer entrance.
- (c) The densities of the gases at different pressures had to be determined for use in cross section calculations.

These and other experimental considerations have been applied to the gas target experiments conducted at the Naval Post-graduate School. So far pure deuterium and hydrogen-deuterium mixtures have been studied by Gaby [Ref.3] and Mader [Ref.4]. Hydrogen-helium mixtures have also been studied and are reported in this thesis.



1. Target Assembly
  2. Coolant Container
  3. Scattering Chamber Cover
  4. Mounting Plate
  5. Leveling Screw
  6. Bellows Assembly
  7. Scattering Chamber
- Scale: 1" = 3"

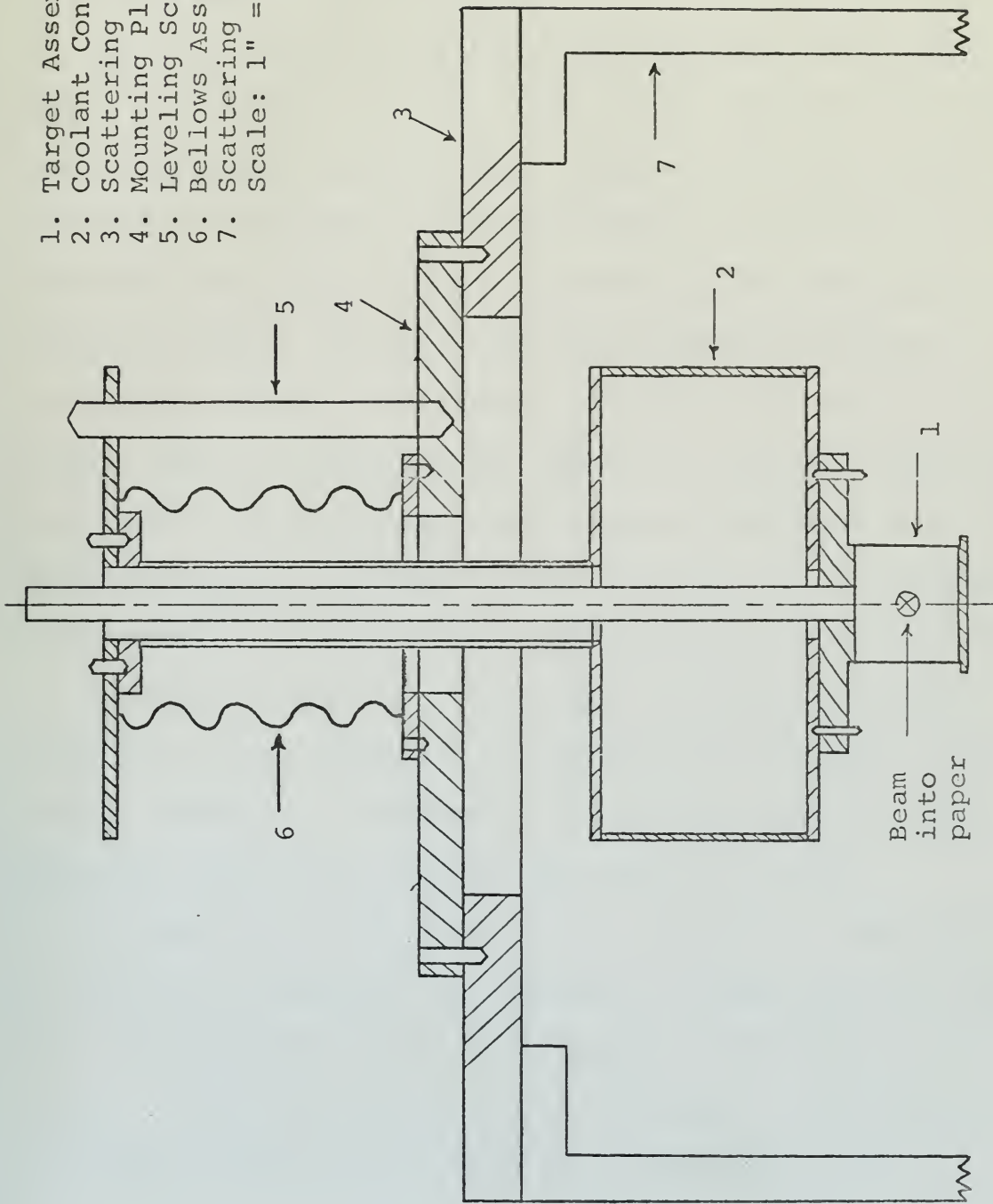


Figure 1. Gas Target Assembly



The purpose of this paper is to provide guidelines for use in further studies of gas targets at NPGLINAC. Data from deuterium and helium experiments were used in preparation of this thesis.

## B. EXPERIMENTAL CALCULATIONS

One of the most important considerations in a cross-section experiment such as a gas target study is the evaluation of radiative corrections. They are of three types: the ionization correction, the Bethe-Heitler correction, and the Schwinger correction. These corrections are described in detail by Gordon [Ref.5]. The experimental problems of target chamber window thicknesses, effective gas target thicknesses, and gas densities all appear in the Bethe-Heitler correction. It was therefore considered constructive to study these parameters and report their significance on experimental outcomes. Likewise, the Schwinger correction was studied for similar reasons. The Schwinger correction has many forms and it was necessary to decide which form was to be used by students. Conformity is important because typical Schwinger corrections are of the order of 10-20%.

In addition to the study of the effects of experimental parameters on radiative corrections, a cross-section experiment was performed using a hydrogen-helium mixture as a target. From the relative cross sections, a calculation of the helium charge form factor as a function of the





four-momentum transfer squared was performed. The results were compared to those obtained at Stanford in 1967 [Ref.6] and to the Gaussian model of the form factor.

## II. RADIATIVE CORRECTIONS

### A. BETHE-HEITLER CORRECTION

The Bethe-Heitler radiative correction was developed to account for part of the tail below a peak in an electron scattering experiment. After incident electrons have scattered off a target nucleus, they lose energy in the form of bremsstrahlung as they pass other nuclei and the atomic electrons of the target nucleus itself. The less energetic electrons are counted at much lower energies than the peak energy, theoretically, all the way to zero energy. It is not possible to set the spectrometer all the way to zero energy because of the length of time involved (the ten-channel system can only monitor an energy range of about three Mev per setting) and the background radiation levels. The Bethe-Heitler correction is an estimate of the number of electrons that should be in the radiative tail due to bremsstrahlung.

Of the different forms of the Bethe-Heitler correction term, the one used was developed by Tsai [Ref.7] and appears in a thesis by Gordon [Ref.5].



$$\delta_B = \left\{ \left[ b_W T_{iW} + 1/2 bt \right] \ln (E_1/\eta^2 \Delta E) + \left[ b_W T_{fW} + 1/2 bt \right] \ln (E_3/\Delta E) \right\} \quad (2-1)$$

where the b's are functions of the atomic number  $Z$  only,

$T_{iW}$  = entrance window thickness

$T_{fW}$  = final window thickness

$t$  = effective target thickness

$E_1$  = incident electron energy

$E_3$  = elastic peak energy

$\Delta E = E_3 -$  (lower limit of electron spectrum)

and  $\eta =$  recoil factor =  $1 + \frac{2E_1}{Mc^2} \frac{\sin^2 \theta}{2}$

where  $M$  = mass of target nucleus

and  $\theta$  = scattering angle.

The Bethe-Heitler correction is applied to the differential cross section in the form  $K_B = e^{-\delta_B}$ . In a ratio experiment using a two-gas mixture, a relative cross section is determined, and the ratio of  $K_B$  for the two gases is entered. The ratio is very nearly equal to one in most cases. The Bethe-Heitler term becomes much more significant in a pure gas experiment. For the hydrogen-helium runs the ratio of the corrections was taken as unity.

In the Bethe-Heitler correction term [Equation 2-1] the important experimental parameters include the window thicknesses and the effective target thicknesses. For this



experiment the window thicknesses of the target chambers were known (1.0 mil stainless steel for the two-inch diameter chamber as well as for the three-inch diameter chamber). The effective target thicknesses were determined from the experimental cross sections, using the assumption that the counting system was 100% effective. The calculations involved the density of the gas in the target chamber. The gas density also appears in the ionization correction term. The virial equation of state was used to calculate gas densities, to take into account deviations from the ideal gas law. The virial equation of state and the method of calculating effective target thicknesses are described in Appendixes B and C.

The effective target thicknesses were calculated for hydrogen and deuterium, using data from the helium runs and Mader's deuterium runs [Ref.4]. The results are shown in Table I.

It was noted from the results that effective target thicknesses were somewhat dependent on energy and very dependent on angle. The effective target thickness was a minimum at  $\theta = 90^\circ$ , and increased in proportion to the deviation of the angle from  $90^\circ$ . For a particular run, the effective target thicknesses of the two gases should have been equal. Discrepancies of from less than 1% up to 10% were noted, however. The deviations were believed to come from the margin of error inherent in calculating the areas under the cross section curves.



TABLE I  
EFFECTIVE TARGET THICKNESS

GAS	RUN <sup>a</sup>	$\theta$	$E_1$ (Mev)	$t_{eff}$ (cm)
H <sub>2</sub>	He1	90°	55.96	.228±.003
H <sub>2</sub>	He2	90°	80.10	.234±.003
H <sub>2</sub>	He3	120°	85.90	.831±.012
H <sub>2</sub>	He4	120°	63.18	.941±.014
H <sub>2</sub>	He5	75°	52.30	.683±.010
H <sub>2</sub>	001	90°	56.82	.274±.004
D <sub>2</sub>	001	90°	56.82	.288±.004
H <sub>2</sub>	004	90°		.225±.004
D <sub>2</sub>	004	90°	85.82	.265±.004
H <sub>2</sub>	006	120°	70.42	.900±.014
D <sub>2</sub>	006	120°		.944±.014
H <sub>2</sub>	009	120°	46.55	.983±.015
D <sub>2</sub>	009	120°		1.03±.015

a: RUNS 001, 004, 006 and 009 were H<sub>2</sub>-D<sub>2</sub> mixtures used by Mader [Ref.4].





Gaby [Ref.3] has used a geometrical approach to calculate effective target thicknesses. The geometrical approach, however, is very idealized and requires many assumptions, so that it is not as reliable as the experimental method.

## B. THE SCHWINGER CORRECTION

The Schwinger radiative correction accounts for energy loss by electrons in the field of the target nucleus, including nuclear bremsstrahlung, virtual photon exchanges, and the emission of photons below the cutoff energy of the cross-section calculations. The Schwinger correction is much larger than the Bethe-Heitler correction for the same experiment, typically ranging from 10% to 20%.

There are several modifications to the original correction developed by Schwinger in 1949 [Ref.8]. The version used in NPGLINAC calculations was put forth by Tsai in 1961 [Ref.9]. The Tsai version of the Schwinger correction is  $K_S = e^{-\delta_S}$ .

$$\delta_S = \frac{2\alpha}{\pi} \left\{ \left[ \frac{1}{2} \ln \frac{E_1}{\eta^2 \Delta E} + \frac{1}{2} \ln \frac{E_3}{\Delta E} - \frac{13}{12} \right] \left[ \ln \frac{q^2 - 1}{m^2 c^2} \right] + \frac{17}{36} \right\} \quad (2-2)$$

where  $\alpha =$  fine structure constant  $= \frac{1}{137}$

$q^2 =$  four-momentum transfer squared (in  $F^{-2}$ )  $= \vec{q}^2 - q_0^2$ .

$m =$  electron mass,

and  $E_1, E_3, \Delta E$  and  $\eta$  are the same quantities that appeared in the Bethe-Heitler correction. The quantity  $\Delta E$  was chosen to be at least four half-widths of the peak of the cross section.



In all the hydrogen-helium runs the half-width was close to 0.25 MeV, so a value of  $\Delta E = 1$  Mev was used in the calculations, not only for the radiative corrections but for determining the areas under the cross-section curves as well.

Tsai also developed a more complicated expression for the Schwinger correction.<sup>1</sup> It is long and difficult to evaluate except by computer. Mader has shown [Ref.4] that for energies obtainable at NPGLINAC, the more complicated Tsai correction did not differ significantly from Equation 2-2. In fact, for gas mixture experiments where only the ratio of the Schwinger corrections for the two gases was needed, the difference in the corrections calculated by the complicated expression and Equation 2-2 was less than 0.1%. Since most of the gas target experiments conducted at NPGLINAC have been performed using gas mixtures, it was considered entirely adequate to use Equation 2-2 to calculate the Schwinger correction terms.

### III. HELIUM FORM FACTOR

#### A. INTRODUCTION

Elastic electron scattering from the  $\text{He}^4$  nucleus has been performed several times, by Hofstadter, et al. [Refs.10,11], by Erich, Frank, Haas and Prange [Ref.12], and by Frosch, McCarthy, Rand and Yearian [Ref.6]. At low values of  $q^2$ , the

---

<sup>1</sup> Equation 3-6 in Ref.5.



charge form factor for  $\text{He}^4$  was found to be in agreement with the Gaussian model:

$$F(q^2) = \exp \left[ -\langle r^2 \rangle q^2 / 6 \right] \quad (3-1)$$

where  $\langle r^2 \rangle$  is the square of the rms radius of the nuclear charge distribution. For  $\text{He}^4$ ,  $\langle r^2 \rangle^{1/2}$  was determined to be 1.63 F by Frank, Haas and Prange [Ref.12]. However, at higher values of  $q^2$  ( $q^2 > 6.2 \text{ F}^{-2}$ ) a deviation from the Gaussian model was discovered. In fact a diffraction zero was found at  $q^2 = 10 \text{ F}^{-2}$  [Ref.6]. A new expression for the  $\text{He}^4$  form factor was obtained on the basis of the experimental work of Frosch, et al.

$$F(q^2) = \left[ 1 - (a^2 q^2)^n \right] \exp(-b^2/q^2) \quad (3-2)$$

with  $n = 6$

$$a = 0.316 \pm 0.001 \text{ F}$$

$$\text{and } b = 0.681 \pm 0.002 \text{ F.}$$

The resulting value of  $\langle r^2 \rangle^{1/2}$  was 1.68 F.

For energies obtainable at NPGLINAC, it was only possible to study the helium form factor at values of  $q^2$  less than  $0.6 \text{ F}^{-2}$ . Therefore it was not possible to distinguish between the two models. A comparison was made to the Gaussian model, however, to help determine the efficiency of NPGLINAC with respect to gas targets in general.



## B. THEORY

Linear accelerators are very useful in producing energetic electrons which can be scattered from nuclei in order to learn something about the charge distributions of the different nucleons and nuclei. The original theories of scattering cross sections were developed by Rutherford and Mott, and assumed that nuclei were point particles. Nuclei are not point particles, however, and their charge distributions have a finite size. In the first Born approximation, the ratio of an experimental cross section to the Mott cross section (including recoil) is called the charge form factor ( $F$ ) and is always less than one for values of  $q^2 > 0$ .

$$\left(\frac{d\sigma}{d\Omega}\right)_{\text{exp}} / \left(\frac{d\sigma}{d\Omega}\right)_{\text{Mott}} = F^2 \quad (3-3)$$

$$\text{where } \left(\frac{d\sigma}{d\Omega}\right)_{\text{Mott}} = \left(\frac{Ze^2}{2E_1}\right)^2 \frac{\cos^2 \frac{\theta}{2}}{\sin^4 \frac{\theta}{2}} \left(\frac{1}{\eta}\right) \quad (3-4)$$

It can be shown that the charge form factor is just the Fourier transform of the charge distribution, and is a function of the momentum transfer:

$$F(K) = \frac{1}{Ze} \iiint \exp(-i\vec{K} \cdot \vec{r}) \rho(\vec{r}) d^3r \quad (3-5)$$

where  $q$  is related to  $K$  by  $q = \hbar K$

For a spinless, spherically symmetric nucleus such as  $\text{He}^4$ , the charge form factor can be expressed as

$$F(K^2) = 1 - \frac{1}{6} K^2 \langle r^2 \rangle + \dots \quad (3-6)$$





A plot of  $F(q^2)$  vs  $q^2$  should have a y-intercept of 1.0 and a slope of  $\frac{-1\langle r^2 \rangle}{6}$ . In this manner the rms radius of the charge distribution can be determined.

### C. EXPERIMENTAL METHOD

#### 1. Procedure

The experiment consisted of using NPGLINAC to scatter electrons from a hydrogen-helium target at different values of  $q^2$  and determining the helium charge form factor from the resulting data. The values of  $q^2$  ranged from  $0.1 \text{ F}^{-2}$  to  $0.55 \text{ F}^{-2}$ . Appropriate angles and machine energies were chosen to give the most reliable data, taking into consideration the energy limitations of the machine, the length of time required for a run, and the background radiation levels.

The data for each run consisted of a spectrum of counts per MeV versus electron energy in MeV. Spectrometer settings were such that the elastic peaks of hydrogen or helium appeared between channels four and five of the ten-channel counting system. The total number of points taken during a run was dependent on the average energy separation between counters. In addition to scanning the helium and hydrogen peaks, a number of points were taken above the helium peak and between the helium and hydrogen peaks in order to obtain measurements of the radiation background levels. The integration of the incident beam was chosen such that at least 10,000 counts were obtained under each peak. The data



for each point, including counts for each of the ten channels, integration capacitance ( $\mu\text{F}$ ) and voltage, time of integration, incident electron energy (MeV) and spectrometer setting (MeV) were recorded on a teletype machine.

## 2. Experimental Errors

Because the experiment involved calculating the ratios of areas under the peaks of helium to hydrogen, systematic errors in the experimental parameters cancelled out. These errors included the deviation of the incident electron beam energy from the set value, which varied less than 0.1% over several hours; the drifting of the magnetic field in the spectrometer, which was held constant to within 1 part in  $10^4$  by a detailed balancing circuit; and changes in the secondary emission monitor (SEM) efficiency. While the absolute SEM efficiency was not critical for evaluating the cross-section ratios, it was more important in determining effective target thicknesses of individual gases.

Statistical errors appeared in both the counting rate and the efficiencies of the counters. The efficiencies of the counters have been measured by Stewart [Ref.13]. With a counting rate of at least 10,000 counts per peak, the statistical error was 1.0% or less.

The largest error was found to occur when evaluating areas under the peaks. This was due to difficulties in determining how much of the radiative tail of helium should be subtracted from the hydrogen peak.



## D. DATA REDUCTION

### 1. Calculation of Cross Sections

The raw data for each run consisted of a teletype printout of counts per channel, incident beam energy, spectrometer setting, and integration data. This data was reduced using a computer program which contained counter efficiencies and the energies "seen" by each of the counters. The reduced data was used to make a plot of energy versus counts per microcoulomb. Two examples of these plots are shown in Figure 2 and Figure 3. They represent values of  $q^2$  of  $0.1031 \text{ F}^{-2}$  and  $0.5496 \text{ F}^{-2}$  and show the different separations of the peaks corresponding to different recoil energies of hydrogen and helium.

The differential cross sections were calculated using the following relation:

$$\left( \frac{d\sigma}{d\Omega} \right)_{\text{exp}} = \frac{N_{\text{sc}}}{N_i N_t \Delta\Omega} \quad (3-7)$$

where  $N_{\text{sc}}$  = number of scattered electrons

$$= \frac{\text{Area under Peak}}{\text{Avg. Energy resolution of counters}} \times \text{Radiative Corrections,}$$

$N_i$  = number of incident electrons,

$N_t$  = number of nuclei per unit area,

and  $\Delta\Omega$  = solid angle subtended by the spectrometer entrance.

It is also known that the experimental cross section equals the Mott cross section ( $\sigma_M$ ) multiplied by the charge form



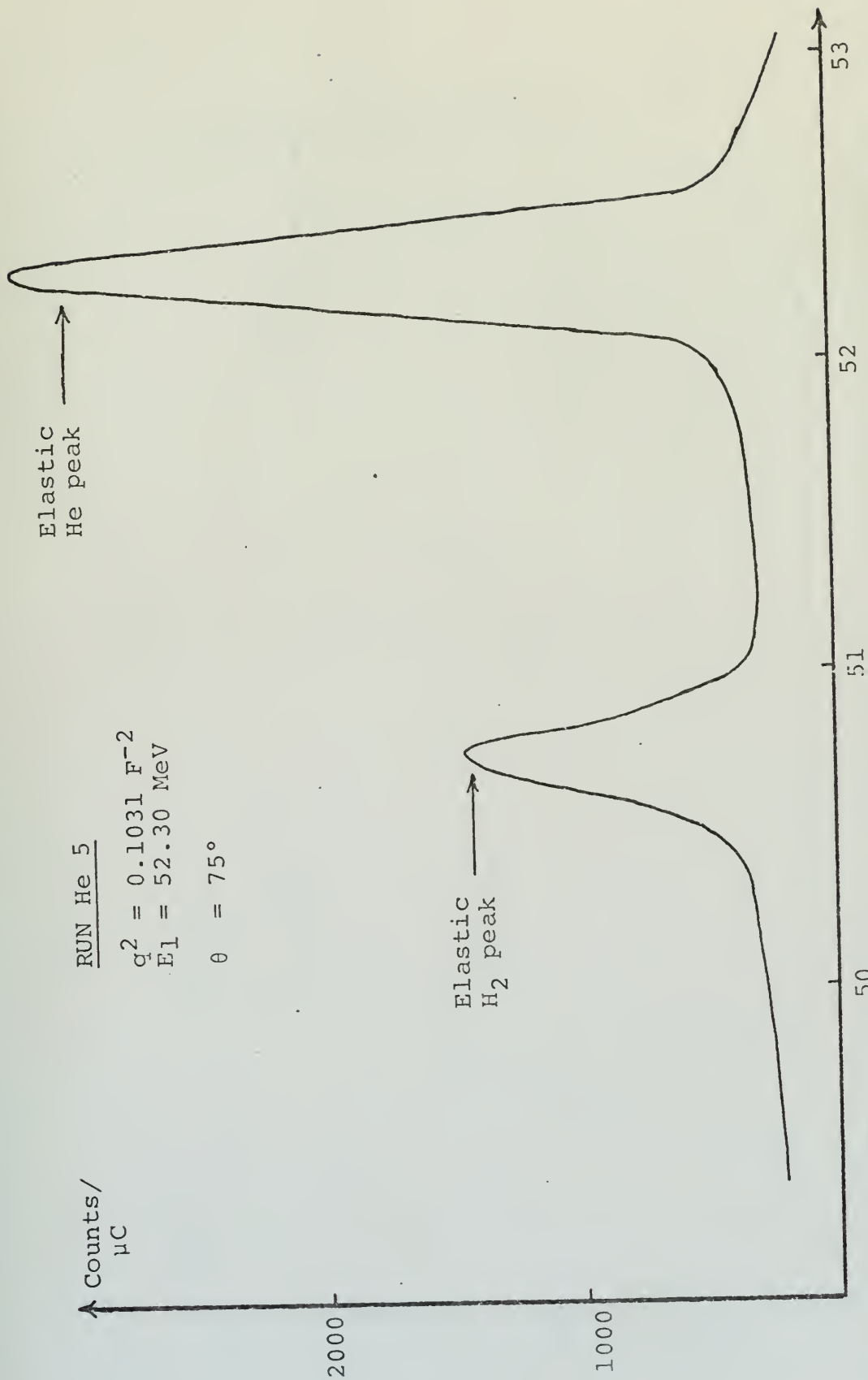


Figure 2. Spectrum of Elastically Scattered Electrons from He - H<sub>2</sub> Gas Mixture





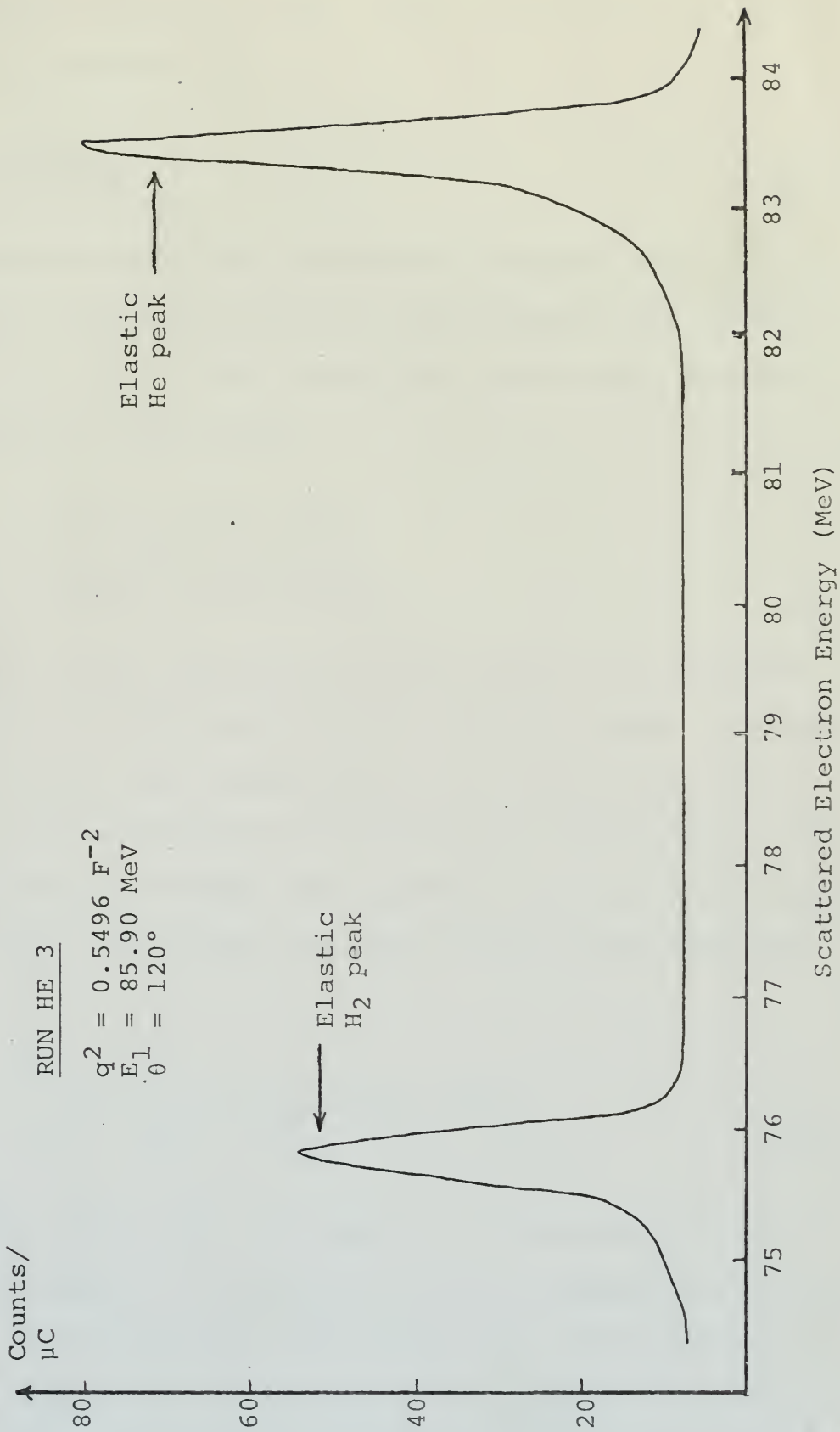


Figure 3. Spectrum of Elastically Scattered Electrons from He - H<sub>2</sub> Gas Mixture



factor squared [Equation 3-3]. Thus the form factor for a gas can be obtained from

$$F^2 = \frac{N_{sc}}{N_i N_t \Delta \Omega \sigma_M} \quad (3-8)$$

In this experiment it was desired to calculate the ratio of the helium charge form factor to the hydrogen form factor.  $N_i$  and  $\Delta \Omega$  fall out of the calculation right away, for they are the same for both gases.

$$\frac{F^2_{He}}{F^2_H} = \frac{(N_{sc})_{He} (N_t)_H (\sigma_M)_H}{(N_{sc})_H (N_t)_{He} (\sigma_M)_{He}} \quad (3-9)$$

The average energy resolution of the counters is directly proportional to the energy of the scattering peak. In this experiment also, the correction for ionization and the Bethe-Heitler correction were the same for both gases. The only radiative correction that appeared then was the Schwinger correction  $K_s$ . Therefore the ratio of the cross sections becomes

$$\frac{F^2_{He}}{F^2_H} = \frac{(A)_{He} (E_3)_H (N_t)_H (\sigma_M)_H (K_s)_H}{(A)_H (E_3)_{He} (N_t)_{He} (\sigma_M)_{He} (K_s)_{He}} \quad (3-10)$$

The areas under the peaks were determined using a three-point method of integration from a prepared calculator program. The appropriate backgrounds were then subtracted out. The upper limit on the energy was chosen to be where the helium curve dropped to background level, which usually



was about 0.3 MeV above the He peak. The lower limit was chosen to be about four half-widths below the peak energy, which was close to 1.0 MeV for all runs. The energy range used for the integrations was essentially the same for both the hydrogen and helium peaks.

The gas concentration  $N_t$  was calculated from the known molar concentrations of  $H_2$  and He. All runs were conducted using a gas mixture that contained 44.9% hydrogen and 55.1% helium. There are two  $H_2$  nuclei for each He nucleus. Thus the ratio of nuclei concentrations was

$$\frac{(N_t)_H}{(N_t)_{He}} = \frac{2(44.9)}{(55.1)} = 1.62976$$

The Mott cross sections were computed from Equation 3-4 using the desk calculator, and the Schwinger radiative corrections were calculated from Equation 2-2. The hydrogen form factors were obtained from a prepared calculator program. Finally, the helium charge form factors were calculated from Equation 3-10.

## 2. Error Analysis

All errors in the calculation of the helium charge form factor were 1.0% or less except for the error in evaluating areas under the cross-section curves. Specifically, it was difficult to determine exactly how much to subtract out from the hydrogen peak due to background and the helium radiative tail. One method used was to take an average background rate between the two peaks and subtract it from the



hydrogen peak. At low values of  $q^2$ , however, the peaks were very close together and this made it difficult to determine an actual background rate [Figure 2]. Another method used was to make a least-squares fit of the helium tail from halfway up the peak to the start of the hydrogen peak. A program was prepared to perform a least-squares fit of the form  $f(x) = a + bx + cx^2$ ,

where  $x_i = \frac{1}{E_0 - E_i}$ ,  $E_0$  being the helium peak energy,

and  $f(x_i) =$  counts per microcoulomb corresponding to energy  $E_i$ . The least-squares fit worked well at low values of  $q^2$ , but at  $q^2 = 0.55 \text{ F}^{-2}$  the quadratic term caused the fit to begin rising under the hydrogen peak. In this case the fit was reduced to  $f(x) = a + bx$  and results were better.

The differences in calculations using an average background rate and a least-squares fit were up to 10%. The method of least squares resulted in form factor values more closely correlated to the expected results. Therefore the least-squares method was used for all calculations in this experiment.

#### E. RESULTS AND CONCLUSIONS

The experimental values of  $F(q^2)$  for each value of  $q^2$  used are listed in Table II and are depicted graphically in Figure 4. The error flags indicate the maximum statistical error of 1.5%. The theoretical curve for a Gaussian potential is also shown for comparison. Although the experimental values of  $F(q^2)$  differed somewhat from the theoretical values





TABLE II  
EXPERIMENTAL He<sup>4</sup> CHARGE FORM FACTOR

RUN	$q^2$ (F <sup>-2</sup> )	(F <sub>He</sub> ) exp	(F <sub>He</sub> ) Gaussian
1	.1585	.982±.015	.9322
2	.3328	.813±.012	.8630
3	.5496	.783±.012	.7840
4	.3000	.815±.012	.8756
5	.1031	.957±.014	.9554



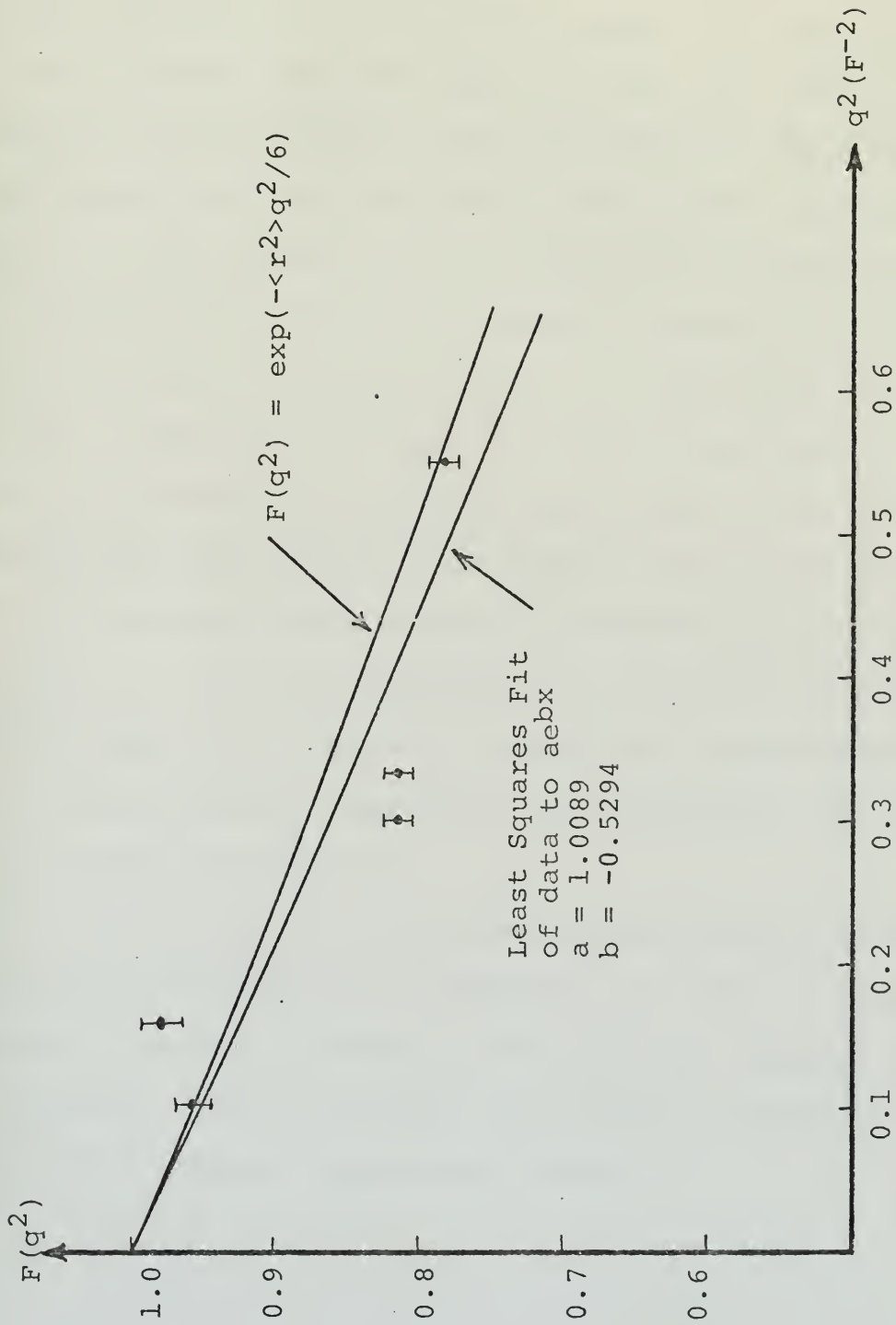


Figure 4. He<sup>4</sup> Charge Form Factor vs. q<sup>2</sup>.



at low values of  $q^2$ , a least-squares fit to the form  $y = ae^{bx}$  produced a curve that nearly coincided with the theoretical curve. The resulting rms radius of the  $\text{He}^4$  nucleus, obtained from the least-squares fit, was  $\langle r^2 \rangle^{1/2} = 1.78 F$ , larger than the expected value by 9.2%. The discrepancies were believed to be due mainly to the difficulties encountered when evaluating areas under the hydrogen peaks. At low values of  $q^2$  the separation between peaks was not wide enough to obtain an accurate determination of background and helium radiative tails. It was noted also that for  $q^2 = .1585 F^{-2}$  the background level increased significantly from the helium peak to the hydrogen peak, causing the experimental form factor to be larger than predicted. At  $q^2 = .55$  however, there was good agreement between experiment and theory. This was believed due to adequate separation between peaks for an accurate background determination, and to a fairly constant background rate throughout the energy range of the calculations.

It is believed that better agreement between helium form-factor experiments at NPGLINAC and those at other laboratories can be obtained by using pure gas targets instead of mixtures. This would ease the burden of attempting to calculate the proper background rates.



APPENDIX A

FREQUENTLY USED CONSTANTS

The following physical constants appeared several times in cross-section calculations and are listed here for future reference:

$$e^2 = 0.144 \times 10^{-12} \text{ MeV} \cdot \text{cm}$$

$$(Mc^2)_H = 938.68 \text{ MeV}$$

$$(Mc^2)_{He} = 3728.01 \text{ MeV}$$

$$\frac{\hbar}{m_e c} = 386.12 \text{ F}$$

$$\frac{2\alpha}{\pi} = 0.46455 \times 10^{-2}$$

$$\frac{1 \text{ cm}^3}{\text{erg}} = 0.68947 \times 10^5 \frac{\text{in.}^2}{\text{lb}}$$

$$RT = 0.643041 \times 10^{10} \frac{\text{erg}}{\text{mole}} \text{ at } T = 77.32^\circ \text{ K}$$

$$1 \frac{\text{dyne}}{\text{cm}^2} = 0.14504 \times 10^{-4} \frac{\text{lb}}{\text{in.}^2}$$





## APPENDIX B

### VIRIAL COEFFICIENTS

The theoretical development of the virial theorem and the virial equation of state is described in Ref.14 and Ref.15. The virial equation of state is an alteration to the ideal gas law ( $pV = nRT$ ) and more accurately describes the properties of real gases. The virial equation of state appears in two forms, a power series expansion in the molar volume and a power series expansion in the pressure. Since pressure is a directly measureable quantity for gas target runs at NPGLINAC, the latter form is more convenient to use:

$$\frac{p\tilde{V}}{RT} = 1 + B'(T)p + C'(T)p^2 + \dots \quad (B-1)$$

$\tilde{V} = \frac{V}{N_0}$ , the molar volume, where  $N_0$  is Avogadro's number.

$$B'(T) = B/RT \text{ and } C'(T) = (C-B^2) / (RT)^2,$$

where  $B$  and  $C$  are the second and third virial coefficients and are functions of temperature only. For the gases currently being studied at Monterey (hydrogen, deuterium and helium) the virial coefficients were calculated from the Lennard-Jones potential for non-polar molecules. Preliminary calculations showed that for a pure gas target, the values of  $B'(T)$  were of the order of  $10^{-3}$  in.<sup>2</sup>/lb and values of  $C'(T)$  were of the order of  $10^{-7}$  in.<sup>2</sup>/lb. The terms involving higher orders of  $p$  were dropped with no significant changes in results.



Evaluation of  $B(T)$  and  $C(T)$  for pure gases is straightforward, using the relations

$$B = b_0 B^*(T^*) \text{ and } C = b_0^2 C^*(T^*).$$

$$b_0 = 2/3\pi N_0 \sigma^2 \text{ cm}^3/\text{mole}, \text{ and } T^* = kT/\epsilon,$$

the reduced temperature.  $\sigma$ ,  $\epsilon/k$  and  $b_0$  are force constants for the Lennard-Jones potential and are tabulated for several gases [Ref.15], including those in use at Monterey. Two values for each parameter are quoted, one determined classically and the other quantum mechanically. The quantum-mechanical parameters are more accurate in principle and were used in all calculations.

Once  $T^*$  has been determined,  $B^*$  and  $C^*$  can be extracted from a table [Ref.15]. For values of  $T^*$  not exactly equal to the tabulated values of  $B^*$  and  $C^*$ , a linear interpolation is necessary to obtain correct values of  $B^*$  and  $C^*$ . Proper substitution yields the quantities  $B'(T)$  and  $C'(T)$ , which can then be entered into the equation of state. All parameters are then known except  $\tilde{V}$ , which is related to the desired parameter  $\rho$  (density) by  $\tilde{V} = \frac{W}{\rho}$ , where  $W$  is the molecular weight. Solving for the density yields the following formula:

$$\rho = \frac{W}{\tilde{V}} = \frac{W_p}{RT [1 + B'(T)p + C'(T)p^2]} \quad (B-2)$$



The calculations of the virial coefficients  $B_{\text{mix}}$  and  $C_{\text{mix}}$  for a gas mixture are slightly more complicated. In fact,  $C_{\text{mix}}$  can not be calculated exactly so it is dropped from the expansion. In general,  $B_{\text{mix}}$  for a gas mixture is given by

$$B_{\text{mix}} = \sum_{i=1}^n \sum_{j=1}^n X_i X_j B_{ij} , \quad (\text{B-3})$$

where  $n$  = number of constituent gases in the mixture and

$X_i$  = molar fraction of the  $i$ th gas in the mixture.

$B_{ij}$  ( $i \neq j$ ) is a theoretical virial coefficient for the gas mixture, where  $T_{ij}^*$  and  $b_0$  are determined from the new parameters  $\epsilon_{ij} = \sqrt{\epsilon_i \epsilon_j}$  and  $\sigma_{ij} = 1/2(\sigma_i + \sigma_j)$ , obtained from the force constants of the  $i$ th and  $j$ th gases in the mixture.

$B_{ij}^*$  is extracted from the table in the same manner as before, only the table is entered with the value

$T_{ij}^* = kT/\epsilon_{ij}$ .  $B_{jj}$  is merely the second virial coefficient for the pure  $j$ th gas in the mixture.

For typically used gas mixtures ( $n = 2$ ), the second virial coefficient becomes

$$B_{\text{mix}} = X_1^2 B_{11} + 2X_1 X_2 B_{12} + X_2^2 B_{22}. \quad (\text{B-4})$$

The temperature of all gases and gas mixtures used at NPGLINAC was the temperature of the liquid nitrogen that was used as a coolant (77.32° K). Variations from this temperature were small during all runs, and it was assumed constant for all calculations. Figure 5 depicts the temperature



bridge control mechanism. Values of the virial coefficients for the gases used are listed in Table III. Table IV shows values of gas densities for typical pressures calculated from the virial equation of state.





TABLE III

VIRIAL COEFFICIENTS FOR SEVERAL GASES AT  $T = 77.32^\circ \text{K}$ 

GAS	$B'(T)$ (in. <sup>2</sup> /lb)	$C'(T)$ (in. <sup>4</sup> /lb <sup>2</sup> )
H <sub>2</sub>	$-.18966 \times 10^{-3}$	$+.12928 \times 10^{-7}$
D <sub>2</sub>	$-.18966 \times 10^{-3}$	$+.12928 \times 10^{-7}$
48.8% H <sub>2</sub> - 51.2% D <sub>2</sub> mixture	$-.18944 \times 10^{-3}$	-----
He	$+.89735 \times 10^{-4}$	$+.71852 \times 10^{-8}$
44.9% H <sub>2</sub> - 55.1% He mixture	$+.43683 \times 10^{-5}$	-----



TABLE IV

DENSITIES OF SEVERAL GASES AT CONSTANT  
TEMPERATURE (77.32° K) FOR VARIOUS PRESSURES

Gas	p (lb/in. <sup>2</sup> )	$\rho$ (gm/cm <sup>3</sup> ) x 10 <sup>-2</sup>
H <sub>2</sub> (in	140	.310906
	148	.329184
	149	.331473
H <sub>2</sub> -D <sub>2</sub> mixture)	150	.333699
	151	.336053
	152	.338344
	160	.356709
D <sub>2</sub> (in	140	.621334
	148	.657862
	149	.662437
H <sub>2</sub> -D <sub>2</sub> mixture)	150	.666885
	151	.671591
	152	.676170
	160	.712871
H <sub>2</sub> (in	140	.302475
	148	.319748
	149	.321907
H <sub>2</sub> -He mixture)	150	.324066
	151	.326225
	152	.328384
	160	.345655
He (in	140	.600643
	148	.634943
	149	.639231
H <sub>2</sub> -He mixture)	150	.643518
	151	.647805
	152	.652093
	160	.686389

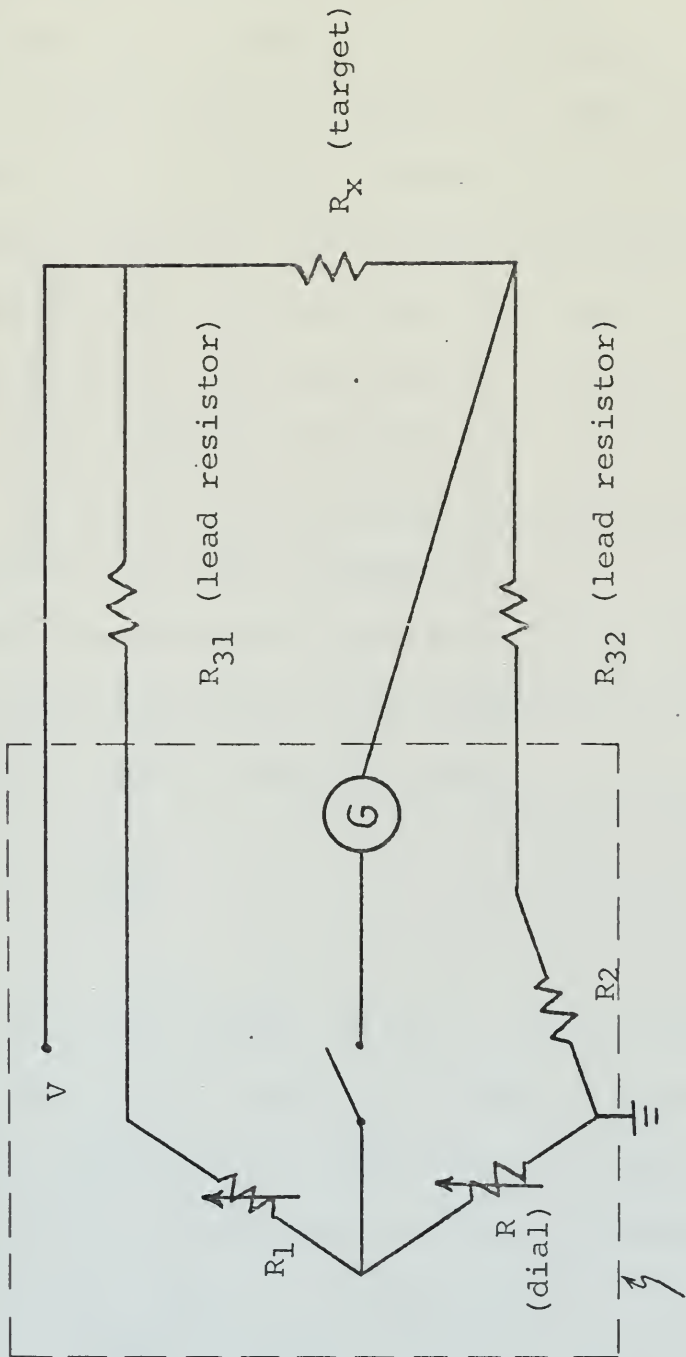


TABLE IV (Cont.)

DENSITIES OF SEVERAL GASES AT CONSTANT  
TEMPERATURE (77.32° K) FOR VARIOUS PRESSURES

Gas	p (lb/in. <sup>2</sup> )	$\rho$ (gm/cm <sup>3</sup> ) $\times 10^{-2}$
H <sub>2</sub> (pure)	140	.310834
	148	.329099
	149	.331386
	150	.333839
	151	.335963
	152	.338252
	160	.356600
D <sub>2</sub> (pure)	140	.621204
	148	.657694
	149	.662264
	150	.667166
	151	.671411
	152	.675986
	160	.712654
He (pure)	140	.593471
	148	.626929
	149	.631108
	150	.635286
	151	.639463
	152	.643640
	160	.677024





Control Panel

$RR_x = \text{constant}$

Figure 5. Temperature Bridge





## APPENDIX C

### GAS TARGET EFFECTIVE THICKNESS

The thickness of a solid target is directly measurable and poses no problem in a cross-section calculation. However, a gas target is different. The pressurized gas is contained in a cylindrical chamber two or three inches in diameter, but only those electrons scattered from a small volume of the gas make their way through the spectrometer entrance slit. The calculation of the effective thickness of a gas target is detailed, and is reviewed here to show what was done for this experiment, and to clarify the procedure for future reference.

The experimental cross section is given by Equation 3-7. The target thickness  $t$  is located in the term  $N_t$ , the number of target nuclei per unit area.

$$N_t = \frac{\rho t N_0}{A} \tag{C-1}$$

where  $A$  is the atomic weight,  $\rho$  is the gas density determined using the virial equation of state, and  $N_0$  is Avogadro's number. Substituting Equation C-1 into Equation 3-7 and solving for  $t$  gives the following expression:

$$t = \left[ \frac{N_{sc}}{\left(\frac{d\sigma}{d\Omega}\right)_{exp} N_i \Delta\Omega} \right] \left[ \frac{A}{\rho N_0} \right] \tag{C-2}$$



$N_{sc}$  is the number of scattered electrons and is equal to the integrated area (counts-MeV) divided by the average resolution of the counters  $\Delta E_r$  (MeV).  $\Delta E_r$  can be calculated from the dispersion formula,

$$\frac{\Delta E_r}{E} = \frac{\Delta p}{p} = \frac{a/r}{D} \quad (C-3)$$

where  $a = 3/16''$

$$r = 16''$$

and  $D = \text{Dispersion factor} = 3.92$ .

Thus  $E_r = 0.00299 E$ .

$$\begin{aligned} \text{The solid angle } \Delta\Omega &= \frac{\text{Area of spectrometer entrance slit}}{r^2} \\ &= \frac{(5/16)(1\ 1/2)}{16^2} \\ &= 0.183 \times 10^{-2} \text{ sr.} \end{aligned}$$

The number of incident electrons is determined from the total charge accumulated in the SEM and the SEM efficiency:

$$N_i = \frac{Q}{e E_{SEM}} \quad (C-4)$$

$e$  is the charge of one electron. The SEM efficiency was assumed constant at 6.1%.

Now the actual integrations calculated from the reduced data were in units of counts per  $\mu\text{C} - \text{MeV}$ . This causes the  $Q$  in  $N_i$  to drop out when  $N_{sc}/N_i$  is calculated:

$$\frac{N_{sc}}{N_i} = \frac{\text{Area} \cdot e \cdot E_{SEM}}{\Delta E_r} \quad (C-5)$$



The experimental cross section is evaluated using Equation 3-3. Thus the final form of the expression for effective target thickness becomes:

$$t = \frac{\text{Area} \cdot e \cdot E_{\text{SEM}} \cdot A}{\sigma_M \cdot \Delta E_r \cdot \Delta \Omega \cdot \rho \cdot N_0}$$
$$= (0.29605 \times 10^{-32}) \left( \frac{\text{Area} \cdot A}{\sigma_M E_\rho} \right) \text{ cm.} \quad (\text{C-6})$$



## LIST OF REFERENCES

1. M.T. Barnett and W.J. Cunnen, Naval Postgraduate School Thesis, 1966.
2. P.N. Midgarden, Naval Postgraduate School Thesis, 1967.
3. L.P. Gaby, Naval Postgraduate School Thesis, 1971.
4. T.W. Mader, Naval Postgraduate School Thesis, 1971.
5. J.A. Gordon, Naval Postgraduate School Thesis, 1970.
6. R.F. Frosch, J.S. McCarthy, R.E. Rand and M.R. Yearian, Phys. Rev. 160, 874 (1967).
7. L.W. Mo and Y.S. Tsai, Rev. Mod. Phys., 41, 205 (1969).
8. J. Schwinger, Phys. Rev., 76, 790 (1949).
9. Y.S. Tsai, Phys. Rev., 122, 1898 (1961).
10. R.W. McAllister and R. Hofstadter, Phys. Rev., 102, 851 (1956).
11. R. Blanckenbecler and R. Hofstadter, Bull. Am. Phys. Soc., 1, 10 (1965).
12. H. Frank, D. Haas and H. Prange, Phys. Letters, 19, 391 (1965).
13. J.W. Stewart, Naval Postgraduate School Thesis, 1970.
14. J.O. Hirschfelder, C.F. Curtiss and R.B. Bird, Molecular Theory of Gases and Liquids (John Wiley and Sons, Inc., New York, 1954), p.2 and p.162.
15. E.U. Condon and H. Odishaw, Ed., Handbook of Physics (McGraw-Hill, New York, 1958), p.5-41.





INITIAL DISTRIBUTION LIST

	No. Copies
1. Defense Documentation Center Cameron Station Alexandria, Virginia 22314	2
2. Library, Code 0212 Naval Postgraduate School Monterey, California 93940	2
3. Assoc Professor F.R. Buskirk, Code 61 Bs Department of Physics Naval Postgraduate School Monterey, California 93940	8
4. Ens. Carter D. Savage, USN 14332 Middletown Lane Westminster, California 92683	1



## DOCUMENT CONTROL DATA - R &amp; D

(Security classification of title, body of abstract and indexing annotation must be entered when the overall report is classified)

1. ORIGINATING ACTIVITY (Corporate author)		2a. REPORT SECURITY CLASSIFICATION	
Naval Postgraduate School Monterey, California 93940		Unclassified	
		2b. GROUP	
3. REPORT TITLE			
Gas Target Studies at the Naval Postgraduate School Linear Accelerator			
4. DESCRIPTIVE NOTES (Type of report and, inclusive dates)			
Master's Thesis (June 1971)			
5. AUTHOR(S) (First name, middle initial, last name)			
Carter D. Savage			
6. REPORT DATE		7a. TOTAL NO. OF PAGES	7b. NO. OF REFS
June 1971		45	15
8a. CONTRACT OR GRANT NO.		9a. ORIGINATOR'S REPORT NUMBER(S)	
b. PROJECT NO.			
c.		9b. OTHER REPORT NO(S) (Any other numbers that may be assigned this report)	
d.			
10. DISTRIBUTION STATEMENT			
Approved for public release; distribution unlimited.			
11. SUPPLEMENTARY NOTES		12. SPONSORING MILITARY ACTIVITY	
		Naval Postgraduate School Monterey, California 93940	
13. ABSTRACT			
<p>A study of the parameters involved in electron scattering experiments with gaseous targets at the Naval Postgraduate School Linear Accelerator was conducted. The parameters included gas densities, effective target thicknesses, and radiative corrections to experimental cross-section calculations. To compare the NPGLINAC with other accelerators, an electron scattering experiment was performed, using a hydrogen-helium gas mixture target, at values of <math>q^2</math> from 0.10 to 0.55 F<sup>-2</sup>. The resulting charge form factor for helium was fairly consistent with previous experimental models; however, it was concluded that experiments using separate gas targets yield greater accuracy than those using a gas mixture.</p>			



KEY WORDS

LINK A

LINK B

LINK C

ROLE

WT

ROLE

WT

ROLE

WT

Electron scattering

Charge form factor

Helium

Radiative corrections

















































































128223

Thesis  
S217  
c.1

Savage

Gas target studies  
at the Naval Post-  
graduate School linear  
accelerator.

128223

Thesis  
S217  
c.1

Savage

Gas target studies  
at the Naval Post-  
graduate School linear  
accelerator.

thesS217

Gas target studies at the Naval Postgrad



3 2768 002 00282 6

DUDLEY KNOX LIBRARY